# Effect of irisin on trabecular bone in a streptozotocin-induced animal model of diabetic osteopathy; a micro-CT study

**Sahar Mohsin** [Corresp., 1], **Fiona Brock** [2], **Suneesh Kaimala** [1], **Charlene Greenwood** [3], **Mohsin Sulaiman** [1], **Keith Rogers** [2], **Ernest Adeghate** [1]

[1] Department of Anatomy, College of Medicine and Health Sciences, United Arab Emirates University, Al Ain, Abudhabi, United Arab Emirates

[2] Cranfield Forensic Institute, Cranfield University, Shrivenham, United Kingdom

[3] School of Chemical and Physical Sciences, Keele University, Newcastle-under-Lyme, Staffordshire, United Kingdom

Corresponding Author: Sahar Mohsin
Email address: smohsin@uaeu.ac.ae

**Background.** Osteoporosis is a significant co-morbidity of diabetes mellitus (DM) leading to increased fracture risk. Exercise-induced hormone 'irisin' in low dosage has been shown to have a beneficial effect on bone metabolism by increasing osteoblast differentiation and reducing osteoclast maturation, and inhibiting apoptosis and inflammation. We investigated the role of irisin in treating diabetic osteopathy by observing its effect on trabecular bone. **Methods.** DM was induced by intraperitoneal injection of streptozotocin 60 mg/kg body weight. Irisin in low dosage (5 µg twice a week for 6 weeks I/P) was injected into half of the control and 4-week diabetic male Wistar rats. Animals were sacrificed six months after induction of diabetes. The trabecular bone in the femoral head and neck was analyzed using a micro-CT technique. Bone turnover markers were measured using ELISA, Western blot, and RT-PCR techniques. **Results.** It was found that DM deteriorates the trabecular bone microstructure by increasing trabecular separation (Tb-Sp) and decreasing trabecular thickness (Tb-Th), bone volume fraction (BV/TV), and bone mineral density (BMD). Irisin treatment positively affects bone quality by increasing trabecular number $p < 0.05$ and improves the BMD, Tb-Sp, and BV/TV by 21-28%. The deterioration in bone microarchitecture is mainly attributed to decreased bone formation observed as low osteocalcin and high sclerostin levels in diabetic bone samples $p < 0.001$. The irisin treatment significantly suppressed the serum and bone sclerostin levels $p < 0.001$, increased the serum CTX1 levels $p < 0.05$, and also showed non-significant improvement in osteocalcin levels. **Conclusions.** This is the first study to our knowledge that shows that irisin marginally improves the trabecular bone in DM most likely by reducing the sclerostin levels.

# Effect of Irisin on trabecular bone in a streptozotocin-induced animal model of diabetic osteopathy; a micro-CT study

Sahar Mohsin[1], Fiona Brock [2], Suneesh Kaimala [1], Charlene Greenwood [3], Mohsin Sulaiman [1], Keith Rogers[2], Ernest Adeghate[1]

[1] Department of Anatomy, College of Medicine and Health Sciences, United Arab Emirates University, Al Ain, United Arab Emirates
[2] Cranfield Forensic Institute, Cranfield University, Shrivenham, UK
[3] School of Chemical and Physical Sciences, Keele University, Staffordshire, UK.

Corresponding Author:
Sahar Mohsin [1]
Khalifa Bin Zayed Street, Tawam, Al Ain, Abu Dhabi, UAE, 15551
Email address: smohsin@uaeu.ac.ae

## Abstract

**Background.** Osteoporosis is a significant co-morbidity of diabetes mellitus (DM) leading to increased fracture risk. Exercise-induced hormone 'irisin' in low dosage has been shown to have a beneficial effect on bone metabolism by increasing osteoblast differentiation and reducing osteoclast maturation, and inhibiting apoptosis and inflammation. We investigated the role of irisin in treating diabetic osteopathy by observing its effect on trabecular bone.

**Methods.** DM was induced by intraperitoneal injection of streptozotocin 60 mg/kg body weight. Irisin in low dosage (5 μg twice a week for 6 weeks I/P) was injected into half of the control and 4-week diabetic male Wistar rats. Animals were sacrificed six months after induction of diabetes. The trabecular bone in the femoral head and neck was analyzed using a micro-CT technique. Bone turnover markers were measured using ELISA, Western blot, and RT-PCR techniques.

**Results.** It was found that DM deteriorates the trabecular bone microstructure by increasing trabecular separation (Tb-Sp) and decreasing trabecular thickness (Tb-Th), bone volume fraction (BV/TV), and bone mineral density (BMD). Irisin treatment positively affects bone quality by increasing trabecular number $p < 0.05$ and improves the BMD, Tb-Sp, and BV/TV by 21-28%. The deterioration in bone microarchitecture is mainly attributed to decreased bone formation observed as low osteocalcin and high sclerostin levels in diabetic bone samples $p < 0.001$. The irisin treatment significantly suppressed the serum and bone sclerostin levels $p < 0.001$, increased the serum CTX1 levels $p < 0.05$, and also showed non-significant improvement in osteocalcin levels.

**Conclusions.** This is the first study to our knowledge that shows that irisin marginally improves the trabecular bone in DM and is an effective peptide in reducing sclerostin levels.

## Introduction

Diabetes mellitus (DM) is associated with increased skeletal fragility, due to a decrease in both bone mineral density (BMD) and altered bone quality (Janghorbani et al. 2006; Janghorbani et al. 2007; Lebiedz-Odrobina & Kay 2010; Napoli et al. 2017). Patients with diabetes mellitus (DM) are at greater risk of fracture due to an increasing tendency to fall not only as a result of peripheral neuropathy, poor vision, and stroke but also due to increased bone loss and/or altered bone matrix and strength (Janghorbani et al. 2006; Mohsin et al. 2019a; Vestergaard 2007).

DM not only affects bone mineral density but also affects bone quality, including bone turnover, microarchitecture, mineralization, microdamage, and bone mineral composition (Hough et al. 2016; Mohsin et al. 2019a; Saito et al. 2006). Animal studies have shown changes in the bone tissue as early as four to eight weeks after the onset of DM (Mohsin et al. 2019a). An increased number of apoptotic osteocytes were found in diabetic rat bones, which explains the imbalance of the remodeling cycle in type 1 diabetes mellitus (DM1). Low levels of serum markers for bone formation such as osteocalcin and bone alkaline phosphatase and increased levels of advanced glycation end products were found in streptozotocin-induced diabetic rats (Hygum et al. 2019; Khan & Fraser 2015; Miyake et al. 2018). Reports on bone resorption in DM are particularly controversial, being reported as unchanged, decreased, or increased in animal and human population studies (Gallacher et al. 1993; Maggio et al. 2010; Motyl & McCabe 2009; Motyl et al. 2009). The major pathogenetic mechanism involved in DM-induced bone deficit is insulin deficiency, along with glucose toxicity, marrow adiposity, inflammation, adipokine, and other metabolic alterations (Hough et al. 2016).

Regular exercise improves the quality of life through its beneficial effects on various systems in the body. Exercise also increases bone and muscle strength and helps prevent bone loss (Benedetti et al. 2018). In turn, increasing physical activity in children with diabetes as well as good glycaemic control appears to provide some improvement in bone parameters (Colberg et al. 2016). Irisin peptide expressed in the skeletal muscle and released after physical activity is reported to increase bone tissue mass and strength (Boström et al. 2012; Colaianni et al. 2015; Khan & Fraser 2015). It can improve insulin resistance, lower blood glucose and promote weight loss. Studies have shown that irisin also helps in cell proliferation and inhibits cell apoptosis (Liu et al. 2017).

The role of irisin in diabetes is still unclear due to contradictory findings (Mahgoub et al. 2018). A recent study (Tentolouris et al. 2018) has shown that circulating irisin levels were lower in subjects with DM1 in comparison with healthy-matched controls. The association of low circulating irisin levels with AGEs accumulation and vascular complications in diabetic patients has been proposed (Rana et al. 2017), and irisin has been reported to have potent anti-inflammatory properties (Mazur-Bialy et al. 2017).

Browning of adipose tissue is reported with a higher irisin dose (3,500 μg. kg−1 per week) but this effect was not seen with low-dose recombinant irisin (r-irisin) in young male mice (Colaianni et al. 2015). More recently it has been shown that irisin in a low dose of 100 μg. $kg^{-1}$ has anabolic effects on bone tissue without browning of adipose tissue. Irisin in low dose modulated the skeletal genes, Opn (osteopontin) and Sost (Sclerostin) (Colaianni et al. 2015; Holmes 2015). Cortical bone

mass and strength were markedly increased in irisin-treated mice, compared with control mice (Colaianni et al. 2015). However, this beneficial effect was only seen in cortical bone and no changes were observed in the trabecular compartment of bone in mice. A marked increase in cortical bone mass was attributed to the suppression of sclerostin which inhibits bone formation through the Wnt signaling pathway, and stimulation of 'osteoblasts' (bone-forming cells) (Colaianni et al. 2015). Moreover, it deters bone resorption by inhibiting osteoclast differentiation (Ma et al. 2018). Due to these actions on bone, irisin is known to enhance the mechanical properties of bone (Gallacher et al. 1993).

Trabecular bone quality is significantly lower in adults with type 1 diabetes (DM1) (Shah et al. 2018) and to our knowledge, the effect of a low dose of irisin on the trabecular bone in DM has not yet been investigated. The study aimed to investigate the role of irisin in ameliorating bone fragility associated with DM, by examining its effect on bone turnover markers and, trabecular bone microstructure using a non-destructive microcomputed tomography (micro-CT) technique in a single high-dose streptozotocin-induced model of diabetes.

## Materials & Methods

### Animal Handling, Induction of Diabetes, and Irisin Treatment

Forty healthy male Wistar rats weighing between, 270 and 300 g were obtained from the Animal House Facility at United Arab Emirates University (UAEU). National Institute of Health (NIH) guidelines for the care and use of laboratory animals were followed for all experiments and procedures carried out in this study after being approved by the Animal Research Ethics Committee of the College of Medicine and Health Sciences, UAE University ERA_2018_5833. The animals were housed singly in cages under standard conditions with a 12 h alternating light and dark cycle, at 22–24 °C and 50–60% humidity, and provided with free access to standard rat chow and water ad libitum during the two weeks of acclimatization and for the experimental period. All efforts were made to minimize animal suffering and to limit the number of animals used (Mohsin et al. 2019a). No adverse event was recorded during the period of the experiment.

A single intraperitoneal (I/P) injection of streptozotocin [STZ, Santa Cruz (U-9889) 60 mg/kg body weight] dissolved in a freshly prepared citrate buffer (0.1 M, pH 4.5) was given to 12 normal Wistar rats to induce experimental diabetes mellitus (Furman 2015). The control rats were injected with equal volumes of the vehicle. Diabetic animals had fasting blood glucose levels of more than 16.7 mmol/l (Mohsin et al. 2019a). Irisin was injected into the treatment groups at 5 µg twice a week for 6 weeks I/P. The animals were euthanized by $CO_2$ overdose (100% $CO_2$ was introduced to the chamber at a fill rate of 50% of the chamber volume per minute) followed by thoracotomy, 6 months after the induction of diabetes. Blood and bones were collected for ELISA, PCR, western blotting, and imaging using micro-CT.

Only 24 animals were used for this pilot study keeping in mind the 3Rs principle to see the effect of irisin if any in treating diabetic osteopathy and the rest of the animals were shared with other researchers in the institution for future studies on other systems.
The experimental animals were equally allocated to different groups at random for treatments and all procedures.
a) Control+vehicle (Gp I Normal untreated NUT)
b) Control+irisin (Gp II Normal treated NT)
c) Diabetic+vehicle (Gp III diabetic untreated DMUT
d) Diabetic+irisin (Gp IV diabetic treated DMT).

They were further subdivided for micro-CT, and bone turnover marker analysis at the end of the experimental period (n=3 to 5) for each analysis. PI and research assistant was aware of the group allocation at different stages of the experiment.

**Data Acquisition Using Microcomputed Tomography**

The bone microarchitecture of the neck of the femur was examined non-invasively using a micro-CT (n=3/Gp). The area of the Ward triangle (Bouxsein et al. 2010b; Courtney et al. 1995) was scanned to detect any early changes in bone mineral density. Each specimen was scanned using a Nikon Metrology XT H225 (X-Tek Systems Ltd, Tring, Hertfordshire, UK) cone-beam μCT scanner operated at 65 kV, and 63 μA, with an exposure time of 1000 ms. The geometric magnification produced a voxel dimension of ca. 23 μm for all the specimens. The software was set to optimize projections (typically 1571), with 2 frames collected per projection. Noise reduction and beam hardening corrections were applied to the data.
To determine the trabecular bone microarchitecture in the femoral head and neck area, bone volume fraction (bone volume/total volume, BV/TV, %), trabecular bone thickness (Tb-Th, mm), trabecular bone separation (Tb-Sp, mm), and trabecular bone number (Tb-N, $mm^{-1}$), the ratio of segmented bone surface to the total volume of the region of interest (BS/BV, $mm^{-1}$), and bone mineral density (BMD, g $cm^{-3}$) were measured using VG Studio Max 2.2 (Volume Graphics GmbH, Heidelberg, Germany) software. All trabecular bone microarchitectural measurements of the femoral head and neck area excluded the cortical bone as in the earlier study (Greenwood et al. 2018).
vTMD values were used to determine volumetric bone mineral density values (vBMD) according to:- vBMD = vTMD × BV/TV. vTMD refers to the density measurement restricted to within the volume of calcified bone tissue, and excludes any surrounding soft tissue, whereas vBMD is the combined density in a well-defined volume (Estell et al. 2020).
A standard BMD phantom (QRM-microCT-HA, QRM GmbH, Moehrendorf, Germany) was used to quantify density within the micro-CT images. The phantom used consists of five cylindrical inserts of known densities of calcium hydroxyapatite (Ca-HA), $Ca10(PO_4)_6(OH)_2$. Proprietary epoxy resin is uniformly filled as the base material. The BMD values of the cylindrical inserts were 1.13 $gcm^{-3}$, 50, 200, 800, and 1200 $mgcm^{-3}$.

**Real-time PCR analysis and Western blots**

Real-time PCR analysis and western blots were carried out in three to four randomly selected rats from each experimental group, to estimate the levels of SOST/sclerostin expression in bone samples at both transcriptional and translational levels. Real-time PCR was carried out by extracting RNA from tibiae by following the trizol method of RNA extraction (Kelly et al. 2014). The high-capacity cDNA reverse transcription kit (Applied Biosystems, 4368813) was used to synthesize cDNA from the extracted RNA. Real-time PCR analysis was performed using the TaqMan primers specific for SOST gene (Thermo Scientific, 4331182) detection and was normalized to β-actin (Thermo Scientific, 4331182) expression levels.

For western blots, 20µg protein extracted from bone samples was separated in a 4-12% SDS-PAGE (Genscript, M00654) and transferred to the PVDF (Polyvinylidene fluoride) blotting membrane. Following blocking with 5% milk in TBST (Tris Buffered Saline with Tween), the membrane was probed using a primary antibody against sclerostin (AF 1589, Mouse SOST/sclerostin antibody, 1:1000 dilution in 5%milk in TBST) and Rabbit anti-goat IgG secondary antibody (Peroxidase conjugated, Cat# A4174, Sigma Aldrich, 1:6000 in TBST). The blots were developed, and the images were captured on an x-ray film. The sclerostin western blot band intensities were normalized to the expression of GAPDH estimated by western blot analysis of the same samples using mouse monoclonal antibody against GAPDH (Sc-32233, Santa Cruz Biotechnology, 1:3000 in 5% milk in TBST) and goat anti-mouse HRP- conjugated secondary antibody (ab205719, 1:5000 in TBST) and shown as relative SOST expression.

**Enzyme-linked Immunosorbent Assay**

ELISA was carried out to estimate the bone turnover markers osteocalcin and C-terminal telopeptide (CTX1) levels in serum and bone samples in three to five randomly selected rats from each experimental group using a readymade kit from Abbkine Scientific (Osteocalcin, KTE1010153) and Cloud-Clone (CTX-1, CEA665Ra) respectively and following the standard manufacturer's protocol. Briefly, 50 µl of the samples or standards were applied to 96 well microtitre plates pre-coated with the ELISA capture antibody, mixed with 50 µl of 1:100 diluted biotin-conjugated competitor and further incubated for 1hr at 37$^{o}$C. The plates were washed thrice with the wash solution, incubated for 30 minutes with 100 µl of 1:100 diluted streptavidin-HRP, and washed five times with the wash solution. The plates were incubated with 90µl of HRP substrate in dark at 37$^{o}$C and the colorimetric reaction was quenched using a stop solution. The absorbance of the plate was measured at 450 nm spectrophotometrically (Tecan Infinite M200 Pro).

**Statistical Analysis**

The data were analyzed using One-way or Two-way ANOVA with Turkey or Bonferroni post-test multiple comparison tests using commercially available software GraphPad Prism 9.0.0 for

Windows, San Diego, California. Adjusted p-value (∗p < 0:05, ∗∗p < 0:01). Data is presented as mean ± standard error (SE).

## Results

**Trabecular bone morphometry using microcomputed tomography (micro-CT)**

Data for all the measured trabecular bone structural parameters and 3D images of the micro-CT scans from each of the four experimental groups are shown in Table 1 and Figure 1 respectively. Plots of changes in various structural parameters of trabecular bone are provided in the supplementary data file [Suppl 1].

**Table 1:** Mean ± S.E between different groups related to trabecular bone parameters obtained using micro-CT. Gp. I—normal un-treated/ NUT, Gp. II— normally treated (NT), Gp. III—diabetic un-treated (DMUT), and Gp. IV—diabetic treated (DMT). Trabecular separation Tb-Sp Gp (I-III = P < 0.05: Trabecular thickness Tb-Th Gp (II-III; II-IV = P <0.05): Trabecular number Tb-N Gp (III-IV = P < 0.05): bone volume/total volume BV/TV Gp (I-III; II-III = P < 0.05): bone surface density BS/ BV Gp (II-III; II-IV P <0.05): Bone mineral density BMD Gp (I-III; II-III = P < 0.05). n=3/Gp.

**Figure 1**: Representation of 3D microarchitecture of the trabecular bone at the proximal end of the femur is shown in frontal (A, C, E, and G) and cross-sectional (B, D, F, and H) images from four groups: A and B (Gp. I—Normal un-treated/ NUT), C & D (Gp. II— Normal treated / NT), E and F (Gp. III—diabetic un-treated / DMUT), and G & H (Gp. IV—diabetic treated / DMT) obtained by using the micro-CT. The image I is the magnified image of (A) to show the region of interest for frontal (red box) and cross-sectional (blue line) images.

The percentage differences for the significant (p < 0.05), and non-significant (p > 0.05) data with a percentage difference of more than 20% for the measured trabecular bone structural parameters are shown in Table 2.

**Table 2:** The percentage differences (%-diff) between different groups for the statistically significant (p < 0.05) data indicated by (*) related to trabecular bone parameters is obtained using micro-CT. Gp. I—normal un-treated/ NUT, Gp. II— normally treated (NT), Gp. III—diabetic un-treated (DMUT), and Gp. IV—diabetic treated (DMT). A high percentage of difference is also found for p > 0.05 data obtained for Tb. Sp Gp III and Gp IV; Tb-Th & between Gp. I and III/ Gp. I and IV; BV/TV Gp III vs GP IV and BMD Gp III vs GP IV.

The mean distance between the trabeculae increased resulting in larger marrow spaces in the diabetic group as seen from the increased trabecular separation and thinning of trabeculae in the untreated diabetic group Gp III-DMUT (Table 1, Figure 1). There was a 59% increase in the

trabecular separation between Gp I-NUT and GP III-DMUT. Irisin treatment decreased the trabecular separation to 28% in the diabetic samples but the change, was not statistically significant ($p > 0.05$) (Table. 2).

The number of trabeculae decreased in GP III-DMUT as compared to Gp I-NUT (Table 1) although not significantly. Treatment with irisin significantly ($p < 0.05$) increased the number of trabeculae in diabetic samples and a 23% difference was recorded (Table 3). Trabecular thickness decreased in diabetes (23%) ) and the irisin treatment did not significantly improve the trabecular thickness (Tables 1 and 2). DM negatively affects BV/TV as can be seen in GP III-DMUT when compared with GP I-NUT and GP II-NT (Table 2). The irisin treatment improved the bone volume by 21.7% (Table 2). BMD significantly decreased in DM; the change was calculated as 39% between the control Gp I-NUT and Gp III-DMUT samples (Table 2). Irisin treatment improved the BMD in the diabetic samples to 27% ($p > 0.05$) (Table 2).

**Effect of irisin on bone turnover markers**

Bone formation decreased significantly in diabetes as indicated by the decreased osteocalcin levels in sera and bone samples in GP- III- DMUT (Figures 2A and 2B).

**Figure 2:** Plots of changes in bone markers in sera and bone tissue is shown (A-E) n= 3-5/Gp; F (n=3-4/Gp): (A) Serum osteocalcin (ng/ml), between GpI and GpIII p=0.0304 (B) Bone osteocalcin (pg/ml) between GpI and GpIII p= 0.0349 (C) Serum CTX1 (ng/ml), between GpI and GpIII p=0.0010 (D) Bone CTX1 (pg/ml), between GpI and GpII p=0.0182, between GpI and GpIII p=0.0094. Relative SOST expression is shown by PCR (E), between GpI and GpII p=0.0078, between GpIII and GpIV p=0.0388 and Western blot (F) between GpI and GpII p= 0.0136, between GpI and GpIII p= 0.0041, between Gp III and GpIV, p= 0.0002 in Gp. I—Normal un-treated/ NUT, Gp. II— Normal treated (NT), Gp. III—diabetic un-treated (DMUT), and Gp. IV—diabetic treated (DMT) compared. Adjusted p-value (∗p < 0:05, ∗∗p < 0:01, ∗∗∗p < 0:001). Error bars = Mean ± SE (western blot uncut image in Suppl data).

Irisin treatment has anabolic action and it improved the osteoblastic activity reflected in raised osteocalcin levels, although the change was not statistically significant. Bone resorption as indicated by measuring CTX-1 in serum and bone samples indicates that resorption increases significantly in diabetes. Treatment with irisin further increased osteoclastic activity and this effect was significant in Gp II (NT) bone samples when compared with those of Gp I (NUT) (Figures 2C and 2D).

We also observed that SOST levels were increased significantly in Gp III (DMUT) compared to Gp I (NUT) bone samples (Figure 2F) $p < 0.01$and were significantly down-regulated with irisin treatment in diabetic samples ($p < 0.01$) in both serum and bone samples (Figure 2E and 2F).

## Discussion

DM1 is associated with poor bone health and a 6-fold increase in the overall incidence of hip fractures (Janghorbani et al. 2006; Janghorbani et al. 2007). Exercise improves many diabetic complications (Colberg et al. 2016). Physical activity induces PGC-1α (peroxisome proliferator-activated receptor-γ co-activator 1α) in the skeletal muscle which is responsible for the synthesis of FNDC5 (fibronectin type III domain-containing protein 5), a membrane protein abundantly expressed in skeletal muscle. Irisin peptide which is obtained by cleavage from its precursor protein FNDC5 is known to be increased post-exercise (Boström et al. 2012).

Irisin levels are significantly inversely correlated with glycated hemoglobin and with years of diabetes (Faienza et al. 2018). Circulating irisin levels were lower in patients with diabetes when compared with healthy-matched controls (Tentolouris et al. 2018). Colaianni et al. (Colaianni et al. 2015; Faienza et al. 2018) have shown that irisin is directly involved in bone metabolism, demonstrating its ability to increase the differentiation of bone marrow stromal cells into mature osteoblasts. Our study investigated the effect of diabetes on trabecular bone microstructure in the proximal femur obtained from mature male Wistar rats using micro-CT and the use of irisin in ameliorating STZ-induced diabetic osteopathy. The study also investigated the change in the bone turnover markers in DM after the irisin treatment. Wistar rats are commonly used in animal research due to similarities in pathophysiologic responses between the human and rat skeleton, combined with the husbandry and financial advantages (Lelovas et al. 2008).

Micro-CT is the most powerful non-invasive technique that has completely revolutionized the assessment of bone architecture *ex vivo*. Micro-CT is the “gold standard technique” for the evaluation of bone microstructure in small animal models. We have previously used micro-CT to analyze the bone microarchitecture in type 2 diabetes in an earlier study (Mohsin et al. 2019b), to investigate trabecular bone microstructure within the head and neck of the femur at a very high resolution without damaging the specimen. The micro-CT reconstructs a 3D representation of the specimen using X-ray attenuation data acquired at multiple viewing angles. The scanning and analyses of data were performed abiding by the published guidelines for assessing bone microstructure in rodents (Bouxsein et al. 2010a)

In this study, the Ward area was also included in the trabecular and BMD measurements. Ward’s triangle is situated at the base of the femoral neck and is regarded as an area of minor resistance. It is defined by the joining of trabeculae of varying lengths and widths depending on the dimensions of the femoral neck which varies with age. The change in bone mineral density occurs early at Ward’s triangle; therefore, evaluation of bone mineral density in this area

contributes to an understanding of femoral neck bone mass distribution and any imbalance is particularly important to assess the risk of bone fragility (Bouxsein et al. 2010b; Furman 2015). DM adversely affects bone tissue making it porous and causing a decrease in bone volume/total volume, an increase in bone turnover (BS/BV), and a significant decrease in BMD (Chen et al. 2018). However, a case-control study comparing the results of iliac biopsies taken from diabetic subjects with those from healthy age- and sex-matched non-diabetic controls found no differences in bone histomorphometric or micro-CT measurements (Armas et al. 2012).

The findings of our study suggest that the distance between the adjacent trabeculae increases significantly within the trabecular bone in a streptozotocin-induced model of diabetes as can be seen from increased Tb-Sp and thinning of trabeculae in Gp III. Increased BS/BV is found in the diabetic groups which show increased osteoclast activity in DM. The number of trabeculae decreased in GP III-DMUT compared to Gp I–NUT, though not significantly. Bone volume fraction (BV/TV) is the percentage ratio of the mineralized bone volume to the total volume of the region of interest in a sample that is negatively affected by DM shown in GP III-DMUT when compared with GP I and GP II normal untreated and treated groups. Trabecular BV/TV is lower in patients who have sustained vertebral and hip fractures (Boutroy et al. 2011; Ciarelli et al. 2000; Legrand et al. 2000; Milovanovic et al. 2012). Similar changes are also seen in age-related bone loss where reduced bone volume is associated with an increase in Tb-Sp and reduced Tb-N. The aging process in both men and women decreases the BV/TV contributing to osteoporosis (Chen et al. 2008). The reduced BV/TV is most likely due to decreases in Tb-N and increases in Tb-Sp which is often found in age-related trabecular bone loss with or without thinning of trabeculae (McCalden et al. 1997; Thomsen et al. 2002).

The trabecular bone strength is dependent on the meshwork of intact trabecular plates of normal width (Thomsen et al. 2002). Treatment with a low dose of irisin 5 μg twice a week for 6 weeks I/P increased the BV/TV by 21.7% in GP IV-DMT irisin-treated group as compared with the saline-treated group (GP III-DMUT). Tb-Sp also decreased (28%) in the GP IV-DMT however the treatment did not improve the Tb-Th or BS/BV in Gp IV-DMT. The number of trabeculae significantly increased with irisin treatment (Gp IV-DMT). It is most likely that irisin results in improved BV/TV due to an increase in trabecular number and reduced trabecular separation. The reduction in the bone volume fraction (BV/TV) is the principal structural alteration observed in the osteoporotic bone a strong correlation between this structural parameter and the overall bone strength has been observed in several studies (Riggs & Parfitt 2005; Thomsen et al. 1998; Zhang et al. 2010).

A measure of bone mineral density (BMD, mg $cm^{-3}$) is important in the evaluation of osteoporosis and other bone-related conditions. Low bone mineral density along with poor bone quality is a risk factor for fragility fractures (Ciarelli et al. 2000; Marshall et al. 1996; Siris et al. 2001; Zhang et al. 2010). In this study, we observed that BMD significantly decreased in the untreated diabetic group of animals and irisin treatment improved the bone mineral density by 27%.

This study did not find a statistically significant change in the trabecular bone parameters in irisin-treated healthy animals in the control group. This is in agreement with a previously published study (Colaianni et al. 2015) which found no change in trabecular bone morphology related to Tb. Th, Tb-N, and Tb-Sp in mice treated with a low dose of r-irisin compared with the control mice. However, that study reported increased cortical bone mineral density and a positive effect on cortical bone geometry following irisin treatment (Colaianni et al. 2015). Nevertheless, a recent study of micro-CT analysis of femurs (Colaianni et al. 2017) showed that r-irisin maintained bone mineral density in both cortical and trabecular bone, and prevented a significant decrease of the trabecular bone volume fraction in hind-limb suspended mice. The thickening of the cortical bones after the irisin treatment is also evident in our experiments(Figures 1D and 1H).

The alteration in the bone microstructure is attributed to changes in the remodeling cycle. Homeostasis in bone requires a balance between bone formation and resorption. Proper vascularisation is indispensable to maintain homeostasis. The skeletal blood vessels were shown to be lined with a highly specialized type of endothelial cells which communicate with the bone cells for a proper course of osteogenesis and bone mineralization (Kusumbe et al. 2016). The impairment of blood supply to the bone tissue as occurs in diabetes could change the proliferation and differentiation of bone precursors in the bone marrow resulting in an altered bone remodeling cycle (Oikawa et al. 2010).

RANK-ligand (RANKL) expressed by osteoblasts activates pre-osteoclasts into mature osteoclasts by binding to receptor activator of nuclear factor-κB (RANK) present on their surfaces (Poole et al. 2005; Wijenayaka et al. 2011). This process is initiated by mechanical forces, which stimulate the release of sclerostin (encoded by the SOST gene) from osteocytes. SOST levels have been reported to increase in DM (Hie et al. 2007; Kim et al. 2015) and they were significantly downregulated with irisin treatment in both normal and diabetic samples in our study. Furthermore, this study is consistent with the earlier reports that sclerostin and irisin are negatively correlated (Colaianni et al. 2015; Klangjareonchai et al. 2014; Zhang et al. 2018) and, in contrast to a study that demonstrated that sclerostin levels increased after giving irisin *in vitro* and *in vivo* (Kim et al. 2018). Sclerostin inhibits osteoblast differentiation through antagonism of the canonical Wnt pathway and inhibits bone formation (Delgado-Calle et al. 2017). SOST upregulates RANKL and down-regulates OPG resulting in stimulating osteoclasts and increased bone resorption (Poole et al. 2005). In osteoclasts, the expression of cathepsin K, TRAP (tartrate-resistant acid phosphatase), and carbonic anhydrase-2 proteins, involved in the remodeling of the extracellular matrix are upregulated by sclerostin (Wijenayaka et al. 2011).

The osteoblastic activity was estimated by measuring the osteocalcin levels in serum and bone samples. The osteocalcin levels significantly decreased in the untreated diabetic samples and treatment with the irisin showed anabolic action and improved the osteoblastic activity by releasing more osteocalcin, although the change was not statistically significant. The suppression of SOST in the treated specimens may have resulted in improving bone formation in the treated samples. The data obtained from this study is consistent with others which also demonstrated

decreased bone formation in diabetes by the significantly decreased level of osteocalcin (Horcajada-Molteni et al. 2001; Li et al. 2005). Hyperglycemia can inhibit osteoblast proliferation and promote osteoclast differentiation, decrease osteocalcin and osteoprotegerin (OPG) expression, promotes calcium loss, and decrease bone mineral density (BMD). r-irisin has been shown by Qiao et al., 2016 to directly act on osteoblast and enhance its proliferation without affecting brown adipose tissue. Irisin treatment increases the expression of osteoblastic transcription regulators and osteoblast differentiation markers by activating the p38 mitogen-activated protein kinase (p38 MAPK) and extracellular signal-regulated kinase (ERK) pathways (Qiao et al. 2016).

Bone resorption was investigated in this study by measuring carboxy-terminal collagen crosslinks (CTX-1) levels in bone and serum samples and consistent with other studies, (Khan & Fraser 2015; Qiao et al. 2016) it was found that bone resorption significantly increases in DM. Further, irisin treatment did not significantly affect the osteoclastic activity in the diabetic samples possibly due to the limited number of samples. A significant change was, however, recorded in the bones of normal rats as irisin treatment further increases the osteoclastic activity as shown by(Ng et al. 2018). Irisin was shown in an earlier study to induce osteoclastogenesis by acting on integrin which, subsequently acts as the receptor for irisin on osteoclasts. Irisin-induced osteoclastogenesis led to the release of carboxy-terminal collagen crosslinks (CTX) and enhanced bone resorption (Kim et al. 2018).

To our knowledge, this is the first study to report the positive effect of irisin on the trabecular bone microstructure in DM. Irisin treatment significantly improves the Tb. N and improves Tb. Sp, BV/TV, and BMD by 22%-28%. The small change could be attributed to a very low dose of irisin and the small number of animals used in this pilot study. The study also found that irisin significantly decreased the sclerostin, anti-anabolic osteokine in diabetic osteopathy.

## Conclusions

The data obtained using a micro-CT analysis corroborates that DM deteriorates the trabecular bone microstructure in the proximal end of the femur which is only partially improved by irisin. Bone formation is adversely affected in STZ-induced diabetic osteopathy which is shown in this study by decreased osteocalcin and increased CTX1 and sclerostin levels. Irisin is a regulator of bone remodeling by acting on all the key players of the bone remodeling cycle. Irisin significantly decreases sclerostin levels in diabetic rats which most likely promotes osteoblast differentiation and bone formation enhancing the trabecular bone quality. However, regarding trabecular bone parameters, statistically significant improvement with the irisin treatment is observed only in the trabecular number. Bone mineral density, bone volume fraction, and trabecular separation improved by 22%-28% only and this could be due to the small sample size and a small dose of irisin used for this pilot study. Conversely, irisin also promotes osteoclastic activity, therefore, would help to treat diabetic osteopathy where low bone turnover is the

underlying pathology. However, the changes reported here with irisin treatment were marginal and further work is required to establish the role of irisin in diabetic osteopathy.

## Acknowledgments

We are grateful to the members of the animal house facility and Ms. Crystal D'souza and Ms. Sara Saeed Dewaib Rahmah Alhmoudi for animal handling at the College of Medicine and Health Sciences, United Arab Emirates University, UAE, Al Ain. Faculty grant, College of Medicine and Health Sciences, United Arab Emirates University, UAE. Grant code and name: G00003027/ NP-19-14. Funders have no role in the design, analysis, and reporting of the study.

### Conflict of interest

The authors declare no potentials conflicts of interest

## References

Armas LA, Akhter MP, Drincic A, and Recker RR. 2012. Trabecular bone histomorphometry in humans with Type 1 Diabetes Mellitus. *Bone* 50:91-96. 10.1016/j.bone.2011.09.055

Benedetti MG, Furlini G, Zati A, and Letizia Mauro G. 2018. The Effectiveness of Physical Exercise on Bone Density in Osteoporotic Patients. *Biomed Res Int* 2018:4840531. 10.1155/2018/4840531

Boström P, Wu J, Jedrychowski MP, Korde A, Ye L, Lo JC, Rasbach KA, Boström EA, Choi JH, Long JZ, Kajimura S, Zingaretti MC, Vind BF, Tu H, Cinti S, Højlund K, Gygi SP, and Spiegelman BM. 2012. A PGC1-α-dependent myokine that drives brown-fat-like development of white fat and thermogenesis. *Nature* 481:463-468. 10.1038/nature10777

Boutroy S, Vilayphiou N, Roux JP, Delmas PD, Blain H, Chapurlat RD, and Chavassieux P. 2011. Comparison of 2D and 3D bone microarchitecture evaluation at the femoral neck, among postmenopausal women with hip fracture or hip osteoarthritis. *Bone* 49:1055-1061. 10.1016/j.bone.2011.07.037

Bouxsein ML, Boyd SK, Christiansen BA, Guldberg RE, Jepsen KJ, and Muller R. 2010a. Guidelines for assessment of bone microstructure in rodents using micro-computed tomography. *J Bone Miner Res* 25:1468-1486. 10.1002/jbmr.141

Bouxsein ML, Boyd SK, Christiansen BA, Guldberg RE, Jepsen KJ, and Müller R. 2010b. Guidelines for assessment of bone microstructure in rodents using micro-computed tomography. *J Bone Miner Res* 25:1468-1486. 10.1002/jbmr.141

Chen H, Shoumura S, Emura S, and Bunai Y. 2008. Regional variations of vertebral trabecular bone microstructure with age and gender. *Osteoporos Int* 19:1473-1483. 10.1007/s00198-008-0593-3

Chen S, Liu D, He S, Yang L, Bao Q, Qin H, Liu H, Zhao Y, and Zong Z. 2018. Differential effects of type 1 diabetes mellitus and subsequent osteoblastic β-catenin activation on

trabecular and cortical bone in a mouse model. *Exp Mol Med* 50:1-14. 10.1038/s12276-018-0186-y

Ciarelli TE, Fyhrie DP, Schaffler MB, and Goldstein SA. 2000. Variations in three-dimensional cancellous bone architecture of the proximal femur in female hip fractures and in controls. *J Bone Miner Res* 15:32-40. 10.1359/jbmr.2000.15.1.32

Colaianni G, Cuscito C, Mongelli T, Pignataro P, Buccoliero C, Liu P, Lu P, Sartini L, Di Comite M, Mori G, Di Benedetto A, Brunetti G, Yuen T, Sun L, Reseland JE, Colucci S, New MI, Zaidi M, Cinti S, and Grano M. 2015. The myokine irisin increases cortical bone mass. *Proc Natl Acad Sci U S A* 112:12157-12162. 10.1073/pnas.1516622112

Colaianni G, Mongelli T, Cuscito C, Pignataro P, Lippo L, Spiro G, Notarnicola A, Severi I, Passeri G, Mori G, Brunetti G, Moretti B, Tarantino U, Colucci SC, Reseland JE, Vettor R, Cinti S, and Grano M. 2017. Irisin prevents and restores bone loss and muscle atrophy in hind-limb suspended mice. *Sci Rep* 7:2811. 10.1038/s41598-017-02557-8

Colberg SR, Sigal RJ, Yardley JE, Riddell MC, Dunstan DW, Dempsey PC, Horton ES, Castorino K, and Tate DF. 2016. Physical Activity/Exercise and Diabetes: A Position Statement of the American Diabetes Association. *Diabetes Care* 39:2065-2079. 10.2337/dc16-1728

Courtney AC, Wachtel EF, Myers ER, and Hayes WC. 1995. Age-related reductions in the strength of the femur tested in a fall-loading configuration. *J Bone Joint Surg Am* 77:387-395. 10.2106/00004623-199503000-00008

Delgado-Calle J, Sato AY, and Bellido T. 2017. Role and mechanism of action of sclerostin in bone. *Bone* 96:29-37. 10.1016/j.bone.2016.10.007

Estell EG, Le PT, Vegting Y, Kim H, Wrann C, Bouxsein ML, Nagano K, Baron R, Spiegelman BM, and Rosen CJ. 2020. Irisin directly stimulates osteoclastogenesis and bone resorption in vitro and in vivo. *Elife* 9. 10.7554/eLife.58172

Faienza MF, Brunetti G, Sanesi L, Colaianni G, Celi M, Piacente L, D'Amato G, Schipani E, Colucci S, and Grano M. 2018. High irisin levels are associated with better glycemic control and bone health in children with Type 1 diabetes. *Diabetes Res Clin Pract* 141:10-17. 10.1016/j.diabres.2018.03.046

Furman BL. 2015. Streptozotocin-Induced Diabetic Models in Mice and Rats. *Curr Protoc Pharmacol* 70:5.47.41-45.47.20. 10.1002/0471141755.ph0547s70

Gallacher SJ, Fenner JA, Fisher BM, Quin JD, Fraser WD, Logue FC, Cowan RA, Boyle IT, and MacCuish AC. 1993. An evaluation of bone density and turnover in premenopausal women with type 1 diabetes mellitus. *Diabet Med* 10:129-133. 10.1111/j.1464-5491.1993.tb00029.x

Greenwood C, Clement J, Dicken A, Evans P, Lyburn I, Martin RM, Stone N, Zioupos P, and Rogers K. 2018. Age-Related Changes in Femoral Head Trabecular Microarchitecture. *Aging Dis* 9:976-987. 10.14336/AD.2018.0124

Hie M, Shimono M, Fujii K, and Tsukamoto I. 2007. Increased cathepsin K and tartrate-resistant acid phosphatase expression in bone of streptozotocin-induced diabetic rats. *Bone* 41:1045-1050. 10.1016/j.bone.2007.08.030

Holmes D. 2015. Bone: Irisin boosts bone mass. *Nat Rev Endocrinol* 11:689. 10.1038/nrendo.2015.174

Horcajada-Molteni MN, Chanteranne B, Lebecque P, Davicco MJ, Coxam V, Young A, and Barlet JP. 2001. Amylin and bone metabolism in streptozotocin-induced diabetic rats. *J Bone Miner Res* 16:958-965. 10.1359/jbmr.2001.16.5.958

Hough FS, Pierroz DD, Cooper C, Ferrari SL, and Group ICBaDW. 2016. MECHANISMS IN ENDOCRINOLOGY: Mechanisms and evaluation of bone fragility in type 1 diabetes mellitus. *Eur J Endocrinol* 174:R127-138. 10.1530/EJE-15-0820

Hygum K, Starup-Linde J, and Langdahl BL. 2019. Diabetes and bone. *Osteoporos Sarcopenia* 5:29-37. 10.1016/j.afos.2019.05.001

572 Janghorbani M, Feskanich D, Willett WC, and Hu F. 2006. Prospective study of diabetes and
573 risk of hip fracture: the Nurses' Health Study. *Diabetes Care* 29:1573-1578.
574 10.2337/dc06-0440
575 Janghorbani M, Van Dam RM, Willett WC, and Hu FB. 2007. Systematic review of type 1 and
576 type 2 diabetes mellitus and risk of fracture. *Am J Epidemiol* 166:495-505.
577 10.1093/aje/kwm106
578 Kelly NH, Schimenti JC, Patrick Ross F, and van der Meulen MC. 2014. A method for isolating
579 high quality RNA from mouse cortical and cancellous bone. *Bone* 68:1-5.
580 10.1016/j.bone.2014.07.022
581 Khan TS, and Fraser LA. 2015. Type 1 diabetes and osteoporosis: from molecular pathways to
582 bone phenotype. *J Osteoporos* 2015:174186. 10.1155/2015/174186
583 Kim H, Wrann CD, Jedrychowski M, Vidoni S, Kitase Y, Nagano K, Zhou C, Chou J, Parkman
584 VA, Novick SJ, Strutzenberg TS, Pascal BD, Le PT, Brooks DJ, Roche AM, Gerber KK,
585 Mattheis L, Chen W, Tu H, Bouxsein ML, Griffin PR, Baron R, Rosen CJ, Bonewald LF,
586 and Spiegelman BM. 2018. Irisin Mediates Effects on Bone and Fat via αV Integrin
587 Receptors. *Cell* 175:1756-1768.e1717. 10.1016/j.cell.2018.10.025
588 Kim JH, Lee DE, Woo GH, Cha JH, Bak EJ, and Yoo YJ. 2015. Osteocytic Sclerostin
589 Expression in Alveolar Bone in Rats With Diabetes Mellitus and Ligature-Induced
590 Periodontitis. *J Periodontol* 86:1005-1011. 10.1902/jop.2015.150083
591 Klangjareonchai T, Nimitphong H, Saetung S, Bhirommuang N, Samittarucksa R,
592 Chanprasertyothin S, Sudatip R, and Ongphiphadhanakul B. 2014. Circulating sclerostin
593 and irisin are related and interact with gender to influence adiposity in adults with
594 prediabetes. *Int J Endocrinol* 2014:261545. 10.1155/2014/261545
595 Kusumbe AP, Ramasamy SK, Itkin T, Mäe MA, Langen UH, Betsholtz C, Lapidot T, and Adams
596 RH. 2016. Age-dependent modulation of vascular niches for haematopoietic stem cells.
597 *Nature* 532:380-384. 10.1038/nature17638
598 Lebiedz-Odrobina D, and Kay J. 2010. Rheumatic manifestations of diabetes mellitus. *Rheum*
599 *Dis Clin North Am* 36:681-699. 10.1016/j.rdc.2010.09.008
600 Legrand E, Chappard D, Pascaretti C, Duquenne M, Krebs S, Rohmer V, Basle MF, and Audran
601 M. 2000. Trabecular bone microarchitecture, bone mineral density, and vertebral
602 fractures in male osteoporosis. J Bone Miner Res 15:13-19. 10.1359/jbmr.2000.15.1.13
603 Lelovas PP, Xanthos TT, Thoma SE, Lyritis GP, Dontas IA.(2008) The laboratory rat as an
604 animal model for osteoporosis research. *Comp Med* 58(5):424-30. PMID: 19004367;
605 PMCID: PMC2707131.
606 Li X, Zhang Y, Kang H, Liu W, Liu P, Zhang J, Harris SE, and Wu D. 2005. Sclerostin binds to
607 LRP5/6 and antagonizes canonical Wnt signaling. *J Biol Chem* 280:19883-19887.
608 10.1074/jbc.M413274200
609 Liu S, Du F, Li X, Wang M, Duan R, Zhang J, Wu Y, and Zhang Q. 2017. Effects and underlying
610 mechanisms of irisin on the proliferation and apoptosis of pancreatic β cells. *PLoS One*
611 12:e0175498. 10.1371/journal.pone.0175498
612 Ma Y, Qiao X, Zeng R, Cheng R, Zhang J, Luo Y, Nie Y, Hu Y, Yang Z, Liu L, Xu W, Xu CC,
613 and Xu L. 2018. Irisin promotes proliferation but inhibits differentiation in osteoclast
614 precursor cells. *FASEB J*:fj201700983RR. 10.1096/fj.201700983RR
615 Maggio AB, Ferrari S, Kraenzlin M, Marchand LM, Schwitzgebel V, Beghetti M, Rizzoli R, and
616 Farpour-Lambert NJ. 2010. Decreased bone turnover in children and adolescents with
617 well controlled type 1 diabetes. *J Pediatr Endocrinol Metab* 23:697-707.
618 10.1515/jpem.2010.23.7.697
619 Mahgoub MO, D'Souza C, Al Darmaki RSMH, Baniyas MMYH, and Adeghate E. 2018. An
620 update on the role of irisin in the regulation of endocrine and metabolic functions.
621 *Peptides* 104:15-23. 10.1016/j.peptides.2018.03.018

622 Marshall D, Johnell O, and Wedel H. 1996. Meta-analysis of how well measures of bone mineral
623 density predict occurrence of osteoporotic fractures. *BMJ* 312:1254-1259.
624 10.1136/bmj.312.7041.1254
625 Mazur-Bialy AI, Pocheć E, and Zarawski M. 2017. Anti-Inflammatory Properties of Irisin,
626 Mediator of Physical Activity, Are Connected with TLR4/MyD88 Signaling Pathway
627 Activation. *Int J Mol Sci* 18. 10.3390/ijms18040701
628 McCalden RW, McGeough JA, and Court-Brown CM. 1997. Age-related changes in the
629 compressive strength of cancellous bone. The relative importance of changes in density
630 and trabecular architecture. *J Bone Joint Surg Am* 79:421-427. 10.2106/00004623-
631 199703000-00016
632 Milovanovic P, Djonic D, Marshall RP, Hahn M, Nikolic S, Zivkovic V, Amling M, and Djuric M.
633 2012. Micro-structural basis for particular vulnerability of the superolateral neck
634 trabecular bone in the postmenopausal women with hip fractures. *Bone* 50:63-68.
635 10.1016/j.bone.2011.09.044
636 Miyake H, Kanazawa I, and Sugimoto T. 2018. Association of Bone Mineral Density, Bone
637 Turnover Markers, and Vertebral Fractures with All-Cause Mortality in Type 2 Diabetes
638 Mellitus. *Calcif Tissue Int* 102:1-13. 10.1007/s00223-017-0324-x
639 Mohsin S, Kaimala S, AlTamimi EKY, Tariq S, and Adeghate E. 2019a. In vivo Labeling of Bone
640 Microdamage in an Animal Model of Type 1 Diabetes Mellitus. *Sci Rep* 9:16994.
641 10.1038/s41598-019-53487-6
642 Mohsin S, Kaimala S, Sunny JJ, Adeghate E, and Brown EM. 2019b. Type 2 Diabetes Mellitus
643 Increases the Risk to Hip Fracture in Postmenopausal Osteoporosis by Deteriorating the
644 Trabecular Bone Microarchitecture and Bone Mass. *J Diabetes Res* 2019:3876957.
645 10.1155/2019/3876957
646 Motyl K, and McCabe LR. 2009. Streptozotocin, type I diabetes severity and bone. *Biol Proced*
647 *Online* 11:296-315. 10.1007/s12575-009-9000-5
648 Motyl KJ, Botolin S, Irwin R, Appledorn DM, Kadakia T, Amalfitano A, Schwartz RC, and
649 McCabe LR. 2009. Bone inflammation and altered gene expression with type I diabetes
650 early onset. *J Cell Physiol* 218:575-583. 10.1002/jcp.21626
651 Napoli N, Chandran M, Pierroz DD, Abrahamsen B, Schwartz AV, Ferrari SL, and Group
652 IBaDW. 2017. Mechanisms of diabetes mellitus-induced bone fragility. *Nat Rev*
653 *Endocrinol* 13:208-219. 10.1038/nrendo.2016.153
654 Ng AY, Tu C, Shen S, Xu D, Oursler MJ, Qu J, and Yang S. 2018. Comparative
655 Characterization of Osteoclasts Derived From Murine Bone Marrow Macrophages and
656 RAW 264.7 Cells Using Quantitative Proteomics. *JBMR Plus* 2:328-340.
657 10.1002/jbm4.10058
658 Oikawa A, Siragusa M, Quaini F, Mangialardi G, Katare RG, Caporali A, van Buul JD, van
659 Alphen FP, Graiani G, Spinetti G, Kraenkel N, Prezioso L, Emanueli C, and Madeddu P.
660 2010. Diabetes mellitus induces bone marrow microangiopathy. *Arterioscler Thromb*
661 *Vasc Biol* 30:498-508. 10.1161/ATVBAHA.109.200154
662 Poole KE, van Bezooijen RL, Loveridge N, Hamersma H, Papapoulos SE, Löwik CW, and
663 Reeve J. 2005. Sclerostin is a delayed secreted product of osteocytes that inhibits bone
664 formation. *FASEB J* 19:1842-1844. 10.1096/fj.05-4221fje
665 Qiao X, Nie Y, Ma Y, Chen Y, Cheng R, Yin W, Hu Y, Xu W, and Xu L. 2016. Irisin promotes
666 osteoblast proliferation and differentiation via activating the MAP kinase signaling
667 pathways. *Sci Rep* 6:18732. 10.1038/srep18732
668 Rana KS, Pararasa C, Afzal I, Nagel DA, Hill EJ, Bailey CJ, Griffiths HR, Kyrou I, Randeva HS,
669 Bellary S, and Brown JE. 2017. Plasma irisin is elevated in type 2 diabetes and is
670 associated with increased E-selectin levels. *Cardiovasc Diabetol* 16:147.
671 10.1186/s12933-017-0627-2

672 Riggs BL, and Parfitt AM. 2005. Drugs used to treat osteoporosis: the critical need for a uniform
673 nomenclature based on their action on bone remodeling. *J Bone Miner Res* 20:177-184.
674 10.1359/JBMR.041114
675 Saito M, Fujii K, Mori Y, and Marumo K. 2006. Role of collagen enzymatic and glycation induced
676 cross-links as a determinant of bone quality in spontaneously diabetic WBN/Kob rats.
677 *Osteoporos Int* 17:1514-1523. 10.1007/s00198-006-0155-5
678 Shah VN, Sippl R, Joshee P, Pyle L, Kohrt WM, Schauer IE, and Snell-Bergeon JK. 2018.
679 Trabecular bone quality is lower in adults with type 1 diabetes and is negatively
680 associated with insulin resistance. *Osteoporos Int* 29:733-739. 10.1007/s00198-017-
681 4353-0
682 Siris ES, Miller PD, Barrett-Connor E, Faulkner KG, Wehren LE, Abbott TA, Berger ML, Santora
683 AC, and Sherwood LM. 2001. Identification and fracture outcomes of undiagnosed low
684 bone mineral density in postmenopausal women: results from the National Osteoporosis
685 Risk Assessment. *JAMA* 286:2815-2822. 10.1001/jama.286.22.2815
686 Tentolouris A, Eleftheriadou I, Tsilingiris D, Anastasiou IA, Kosta OA, Mourouzis I, Kokkinos A,
687 Pantos C, Katsilambros N, and Tentolouris N. 2018. Plasma Irisin Levels in Subjects
688 with Type 1 Diabetes: Comparison with Healthy Controls. *Horm Metab Res* 50:803-810.
689 10.1055/a-0748-6170
690 Thomsen JS, Ebbesen EN, and Mosekilde L. 1998. Relationships between static
691 histomorphometry and bone strength measurements in human iliac crest bone biopsies.
692 *Bone* 22:153-163. 10.1016/s8756-3282(97)00235-4
693 Thomsen JS, Ebbesen EN, and Mosekilde LI. 2002. Age-related differences between thinning of
694 horizontal and vertical trabeculae in human lumbar bone as assessed by a new
695 computerized method. *Bone* 31:136-142. 10.1016/s8756-3282(02)00801-3
696 Vestergaard P. 2007. Discrepancies in bone mineral density and fracture risk in patients with
697 type 1 and type 2 diabetes--a meta-analysis. *Osteoporos Int* 18:427-444.
698 10.1007/s00198-006-0253-4
699 Wijenayaka AR, Kogawa M, Lim HP, Bonewald LF, Findlay DM, and Atkins GJ. 2011. Sclerostin
700 stimulates osteocyte support of osteoclast activity by a RANKL-dependent pathway.
701 *PLoS One* 6:e25900. 10.1371/journal.pone.0025900
702 Zhang D, Bae C, Lee J, Jin Z, Kang M, Cho YS, Kim JH, Lee W, and Lim SK. 2018. The bone
703 anabolic effects of irisin are through preferential stimulation of aerobic glycolysis. *Bone*
704 114:150-160. 10.1016/j.bone.2018.05.013
705 Zhang ZM, Li ZC, Jiang LS, Jiang SD, and Dai LY. 2010. Micro-CT and mechanical evaluation
706 of subchondral trabecular bone structure between postmenopausal women with
707 osteoarthritis and osteoporosis. *Osteoporos Int* 21:1383-1390. 10.1007/s00198-009-
708 1071-2
709

# Figure 1

Representation of 3D microarchitecture of the trabecular bone

Representation of 3D microarchitecture of the trabecular bone at the proximal end of the femur is shown in frontal (A, C, E, and G) and cross-sectional (B, D, F, and H) images from four groups: A and B (Gp. I—Normal un-treated/ NUT), C & D (Gp. II— Normal treated / NT), E and F (Gp. III—diabetic un-treated / DMUT), and G & H (Gp. IV—diabetic treated / DMT) obtained by using the micro-CT. Image I is the magnified image of (A) to show the region of interest for frontal (red box) and cross-sectional (blue line) images.

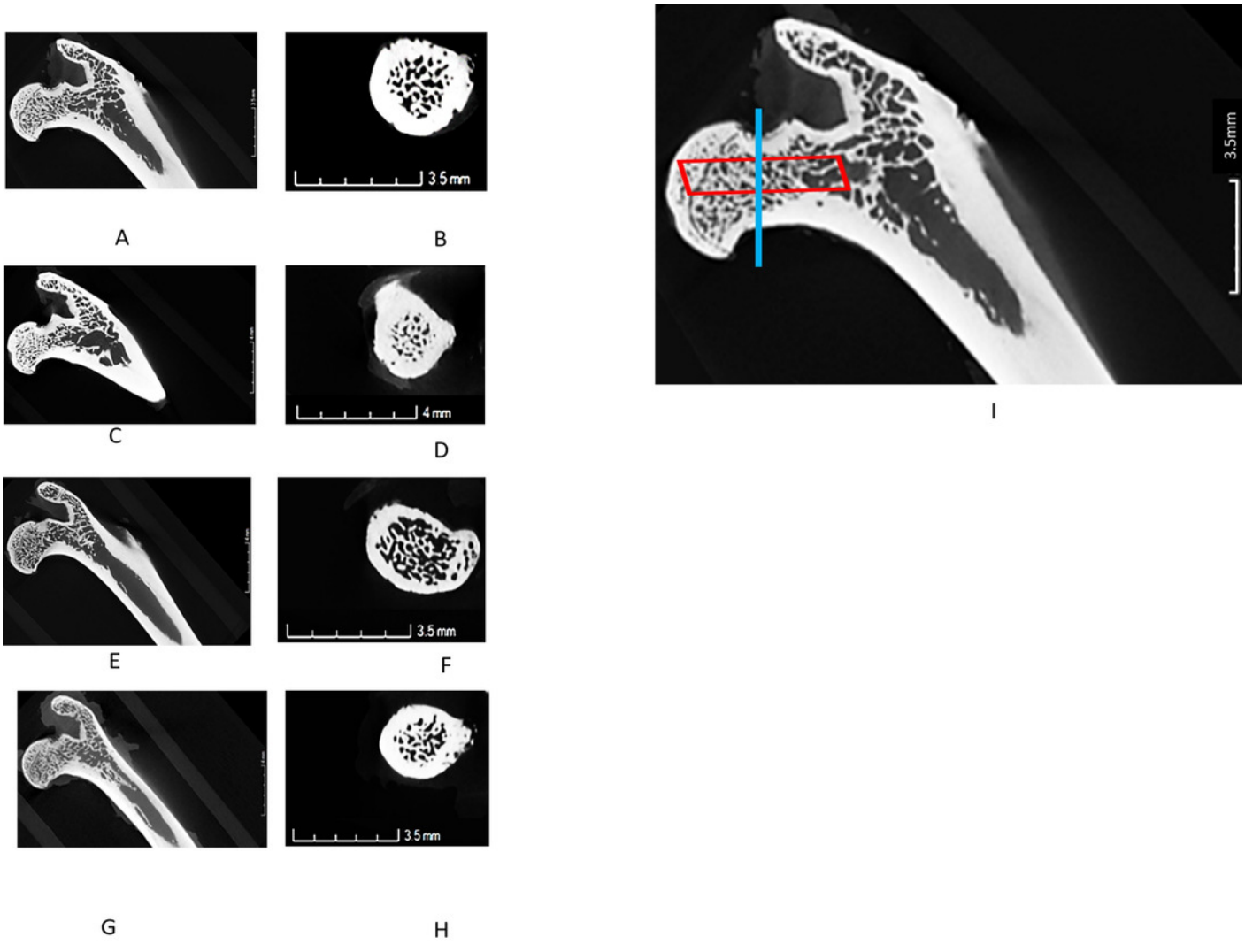

# Figure 2

Plots of changes in bone markers in sera and bone tissue

Plots of changes in bone markers in sera and bone tissue is shown (A-E) n= 3-5/Gp; F (n=3-4/Gp): (A) Serum osteocalcin (ng/ml), between GpI and GpIII p=0.0304 (B) Bone osteocalcin (pg/ml) between GpI and GpIII p= 0.0349 (C) Serum CTX1 (ng/ml), between GpI and GpIII p=0.0010 (D) Bone CTX1 (pg/ml), between GpI and GpII p=0.0182, between GpI and GpIII p=0.0094. Relative SOST expression is shown by PCR (E), between GpI and GpII p=0.0078, between GpIII and GpIV p=0.0388 and Western blot (F) between GpI and GpII p= 0.0136, between GpI and GpIII p= 0.0041, between Gp III and GpIV, p= 0.0002 in Gp. I—Normal un-treated/ NUT, Gp. II— Normal treated (NT), Gp. III—diabetic un-treated (DMUT), and Gp. IV—diabetic treated (DMT) compared. Adjusted p-value (∗p < 0:05, ∗∗p < 0:01, ∗∗∗p < 0:001). Error bars = Mean ± SE

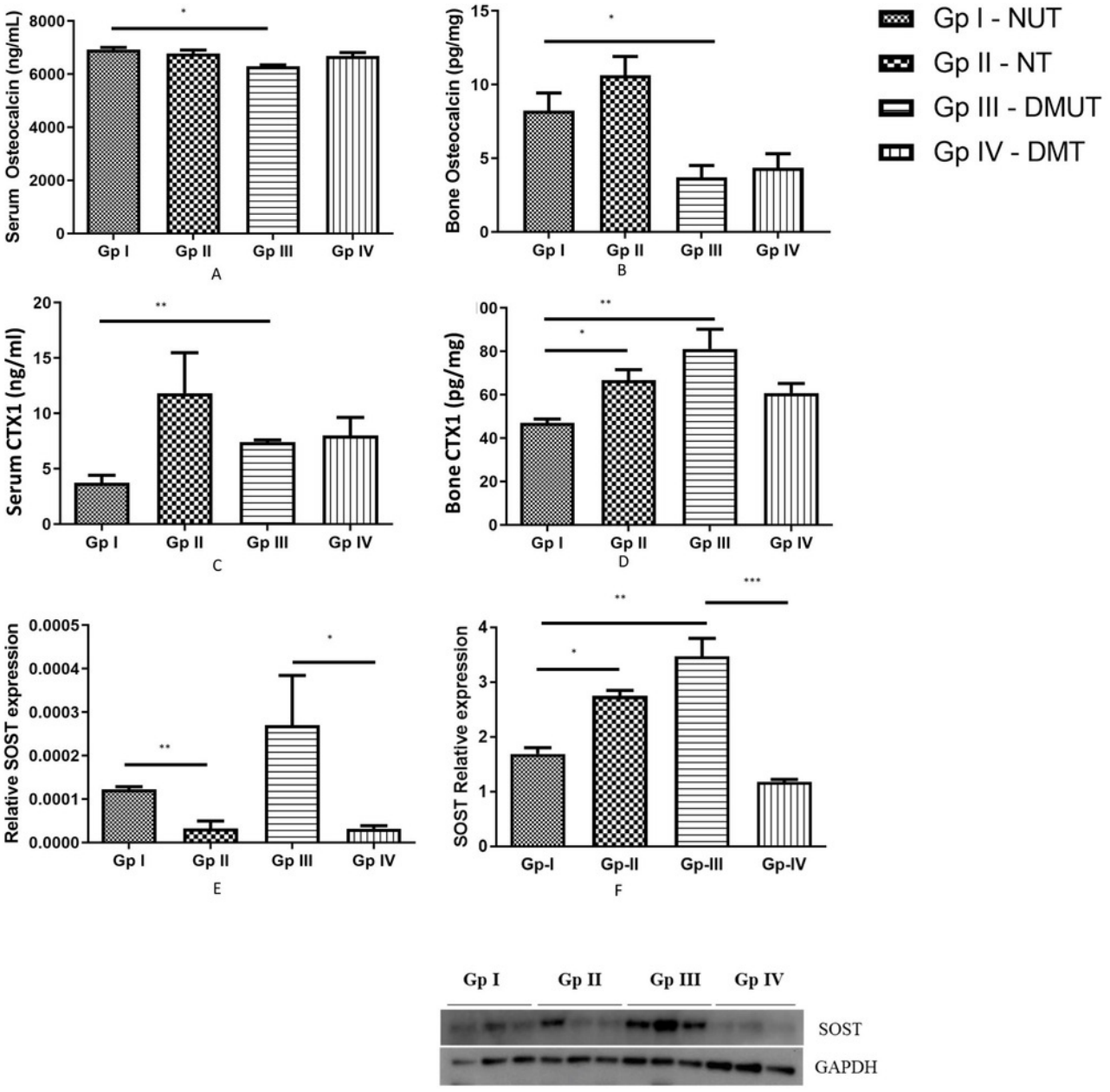
Gp I - NUT
Gp II - NT
Gp III - DMUT
Gp IV - DMT
Serum Osteocalcin (ng/mL)
Bone Osteocalcin (pg/mg)
Serum CTX1 (ng/ml)
Bone CTX1 (pg/mg)
Relative SOST expression
SOST Relative expression
Gp I
Gp II
Gp III
Gp IV
Gp-I
Gp-II
Gp-III
Gp-IV
A
B
C
D
E
F
SOST
GAPDH

## Table 1(on next page)

Mean ± S.E between different groups related to trabecular bone parameters

Mean ± S.E between different groups related to trabecular bone parameters obtained using micro-CT. Gp. I—normal un-treated/ NUT, Gp. II— normally treated (NT), Gp. III—diabetic un-treated (DMUT), and Gp. IV—diabetic treated (DMT). Trabecular separation Tb-Sp Gp (I-III = $P < 0.05$: Trabecular thickness Tb-Th Gp (II-III; II-IV = $P < 0.05$): Trabecular number Tb-N Gp (III-IV = $P < 0.05$): bone volume/total volume BV/TV Gp (I-III; II-III = $P < 0.05$): bone surface density BS/ BV Gp (II-III; II-IV $P < 0.05$): Bone mineral density BMD Gp (I-III; II-III = $P < 0.05$). n=3/Gp.

| Parameters | Mean ± S.E in the experimental Groups | | | |
|---|---|---|---|---|
| | Gp. I | Gp. II | Gp. III | Gp. IV |
| Tb-Sp (mm) | 0.09867 ± 0.007781 | 0.1079 ±0.01554 | 0.1570 ± 0.008653 | 0.1137± 0.008182 |
| Tb-Th (mm) | 0.1051 ± 0.007647 | 0.1189 ±0.01297 | 0.0803 ± 0.008294 | 0.0789 ± 0.002389 |
| Tb-N (1/mm) | 4.910 ± 0.08251 | 4.422 ± 0.1725 | 4.243 ± 0.2492 | 5.222 ± 0.2683 |
| BV/TV % | 0.5159 ± 0.03683 | 0.5255 ± 0.05855 | 0.3376 ± 0.02096 | 0.4109 ± 0.01061 |
| BS/BV 1/mm | 19.24 ± 1.478 | 17.19 ± 1.704 | 25.39 ± 2.427 | 25.39 ± 0.7572 |
| BMD g/cm² | 0.7527 ± 0.05921 | 0.7847 ± 0.1022 | 0.4580 ± 0.04238 | 0.5820 ± 0.02126 |

1

2

## Table 2(on next page)

The percentage differences (%-diff) between different groups

The percentage differences (%-diff) between different groups for the statistically significant ($p < 0.05$) data indicated by (*) related to trabecular bone parameters is obtained using micro-CT. Gp. I—normal un-treated/ NUT, Gp. II— normally treated (NT), Gp. III—diabetic un-treated (DMUT), and Gp. IV—diabetic treated (DMT). A high percentage of difference is also found for $p > 0.05$ data obtained for Tb. Sp Gp III and Gp IV; Tb-Th & between Gp. I and III/ Gp. I and IV; BV/TV Gp III vs GP IV and BMD Gp III vs GP IV.

| Parameters | % Differences between the experimental Groups(* indicates P<0.05) | | | |
|---|---|---|---|---|
| **Tb-Sp (mm)** | Gp I vs Gp III *59%↑ | Gp II vs Gp III *45.5%↑ | Gp III vs GP IV 28%↓ (N.S) | |
| **Tb-Th (mm)** | Gp I vs Gp III 23%↓ | Gp I vs Gp IV 25% ↓ | Gp II vs Gp III *32.5%↓ | Gp II vs Gp IV *33.6%↓ |
| **Tb-N (1/mm)** | Gp III vs GP IV *23% ↑ | | | |
| **BV/TV %** | Gp I vs Gp III *34.5% ↓ | Gp II vs Gp III *35.7%↓ | Gp III vs GP IV 21.7% (N.S)↑ | |
| **BS/BV 1/mm** | Gp II vs Gp III *47.7% ↑ | Gp II vs Gp IV *47.7% ↑ | Gp I vs Gp III 31.96%↑ | |
| **BMD g/cm$^2$** | Gp I vs Gp III *39%↓ | Gp II vs Gp III *42% ↓ | Gp III vs GP IV 27%↑ | |

1